JMEPEG
DOI: 10.1007/s11665-008-9292-7

1059-9495/$19.00

Intermetallic Compounds Formed in Sn-20In-2.8Ag Solder BGA Packages with Ag/Cu Pads

C.C. Jain, S.S. Wang, K.W. Huang, and T.H. Chuang

(Submitted January 24, 2008; in revised form July 11, 2008)

The interfacial reactions in a Sn-20In-2.8Ag solder ball grid array (BGA) package with immersion Ag surface finish are investigated. After reflow, the Ag thin film dissolves quickly into the solder matrix, and scallop-shaped intermetallic layers, with compositions of $(Cu_{0.98}Ag_{0.02})_6(In_{0.59}Sn_{0.41})_5$, appear at the interfaces between Sn-20In-2.8Ag solder ball and Cu pad. No evident growth of the $(Cu_{0.98}Ag_{0.02})_6(Sn_{0.59}In_{0.41})_5$ intermetallic compounds was observed after prolonged aging at 100 °C. However, the growth accelerated at 150 °C, with more intermetallic scallops floating into the solder matrix. The intermetallic thickness versus the square root of reaction time ($t^{1/2}$) shows a linear relation, indicating that the growth of intermetallic compounds is diffusion-controlled. Ball shear tests show that the strength of Sn-20In-2.8Ag solder joints after reflow is 4.4 N, which increases to 5.18 N and 5.14 N after aging at 100 and 150 °C, respectively.

Keywords BGA package, immersion Ag surface finish, interfacial reactions, Sn-20In-2.8Ag

1. Introduction

In order to prevent oxidation and promote the wettability of a printed circuit board, many surface finishing techniques have been explored, among which the immersion Au/Ni method is popularly employed in advanced electronic packaging (Ref 1). However, this method is costly and in some cases can cause Au embrittlement failure (Ref 2). Immersion Ag is an alternative surface finishing agent, which can provide smooth surfaces and good wettability for liquid solders on Cu pads (Ref 3). In addition, the process involving immersion Ag takes about 7 min, and the cost is close to those with traditional Sn surface finishes. An immersion Ag film is about 0.2 μm thick and dissolves quickly into the solder matrix during reflow, allowing further interfacial reaction to occur between the solder alloy and the Cu pad.

Sn-3.5Ag solder possesses the merits of high strength, improved creep resistance, longer fatigue life, and good wettability (Ref 4). However, the high melting temperature (221 °C) of this eutectic alloy hastens the dissolution of the Cu pad into the liquid solder and results in the rapid growth of intermetallic compounds. Also, commonly used FR-4 printed circuit boards can be damaged during very high temperature reflow. Sn-20In-2.8Ag solder has been developed to solve this problem by adding the element indium to lower the melting points and increase the wettability (Ref 5). Shimizn et al. further indicated that indium-based solders possess a more durable fatigue life than Pb-Sn solders and are well suited for high reliability interconnections (Ref 6). The interfacial reactions of Sn-20In-2.8Ag solders with Ni and Ag substrates have been investigated, which led to the formation of $Ni_3(Sn_{0.99}In_{0.01})_4$ and $Ag_2(In,Sn)$ intermetallic compounds, respectively (Ref 7, 8). The intermetallic reactions in Sn-20In-2.8Ag solder ball grid array (BGA) packages with Au/Ni/Cu pads have also been previously investigated (Ref 9), revealing the formation of $Ni(Sn_{0.72}In_{0.28})_2$ phase at the solder/pad interfaces after the reflowing process and aging at 100 °C. However, after aging at a higher temperature of 150 °C, many column-shaped $(Cu_{0.74}Ni_{0.26})_6(Sn_{0.92}In_{0.08})_5$ intermetallics grew rapidly from the solder/pad interface into the solder matrix (Ref 9). Although immersion Ag has become popular for surface finishing of Cu pads in electronic packaging, the intermetallic compounds formed in such solder joints are scantily researched. The effort of this study is concerned with the interfacial reactions of Sn-20In-2.8Ag solder balls with Ag/Cu pads in reflowed and aged BGA packages, as well as the effect of immersion Ag on the shear strength of the solder joints.

2. Experimental

The BGA package used in this study contained 49 Cu pads set on each FR-4 substrate. The Cu pads were immersion-plated with 0.2 μm thick Ag film. The Sn-20In-2.8Ag solder balls, with diameters of 0.4 mm, were dipped in RMA type flux, placed on the immersion Ag/Cu pads of the BGA packages, and then heated in a hot-air furnace. The solidus and liquidus of Sn-20In-2.8Ag as analyzed by DSC (see Fig. 1) are 176.3 and 187.7 °C, respectively. The reflow temperature profile with a peak temperature at 230 °C for a melting time of 60 s ($T > 176.3$ °C) is shown in Fig. 2. After reflow, the specimens were further aged at 100 and 150 °C for durations varying from 100 to 1000 h. To investigate the metallographic microstructure, the solder joints were mounted with resin and then ground

C.C. Jain, S.S. Wang, K.W. Huang, and **T.H. Chuang**, Department of Materials Science and Engineering, National Taiwan University, Taipei 106, Taiwan. Contact e-mail: tunghan@ntu.edu.tw.

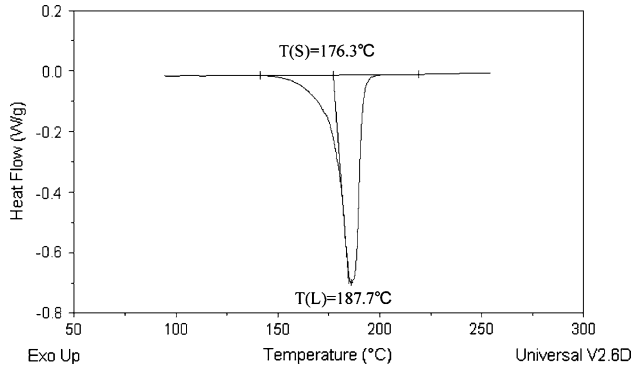

Fig. 1 Solidus and liquidus of Sn-20In-2.8Ag solder as shown in the DSC curve

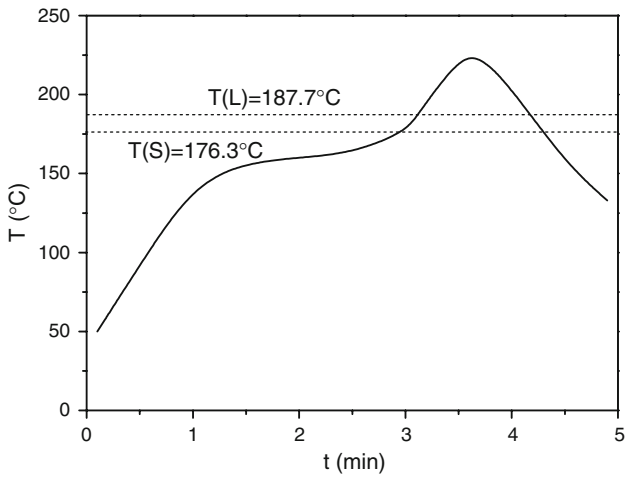

Fig. 2 Temperature profile for the reflowed Sn-20In-2.8Ag BGA packages within this study

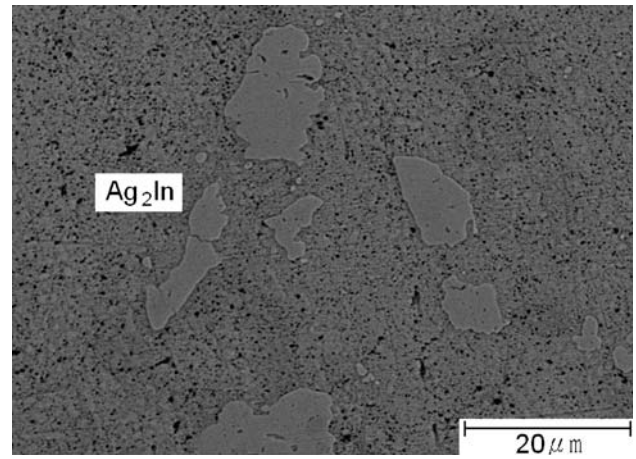

Fig. 3 Microstructure of the as-cast Sn-20In-2.8Ag solder matrix on Ag immersion surface finished pads

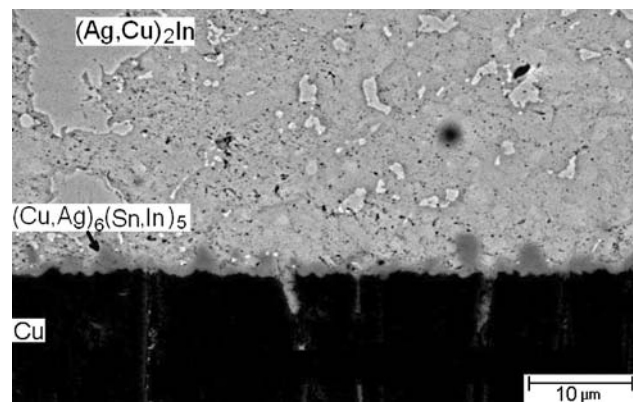

Fig. 4 Morphology of the intermetallic compounds formed at the immersion Ag surface finished interface of reflowed Sn-20In-2.8Ag solder BGA packages

with 1500 grit SiC paper and polished with 0.3 μm Al_2O_3 powder in order to obtain the crosssections of the solder/pads interfaces. The morphology of the intermetallic compounds was examined via scanning electron microscopy (SEM). Energy dispersive X-ray (EDX) spectrometry was used to determine the chemical composition of the intermetallic compounds.

In addition, the bonding strengths of the Sn-20In-2.8Ag solder joints after reflow and aging were measured via ball shear testing. The measurements were taken at a shear rate of 0.1 mm/s and a shear height of 80 μm (about 1/4 of the reflowed ball height). Fractography of the solder joints after ball shear testing was conducted by SEM.

3. Results and Discussion

The typical microstructure of the as-cast Sn-20In-2.8Ag alloy is shown in Fig. 3, where a great number of island-like Ag_2In precipitates are embedded in the Sn-rich matrix. After reflow, the Ag thin film dissolves quickly, and scallop-shaped intermetallic compounds appear at the interface between Sn-20In-2.8Ag solder balls and the immersion Ag/Cu pad, as shown in Fig. 4. The chemical composition (at.%) of the intermetallic layer as analyzed by EDX is Cu:Ag:Sn:In = 55.46:1.08:28.52:14.94, which corresponds to the η-$(Cu_{0.98}Ag_{0.02})_6(Sn_{0.59}In_{0.41})_5$ phase. The formation of such η-$(Cu_{0.98}Ag_{0.02})_6(Sn_{0.59}In_{0.41})_5$ intermetallics is due to the dissolution of Ag thin film and the interfacial reactions between Sn-20In-2.8Ag solder and Cu pad. However, the Cu pad also dissolves into the solder matrix to cause the change of the composition of island-like Ag_2In precipitates to Ag:Cu:In = 63.66:3.85:32.49, which corresponds to the $(Ag_{0.94}In_{0.06})_2In$ phase.

In the prior study, coarse Ag_3Sn plates were observed during the soldering reaction of liquid Sn and Sn-3.5Ag with the Ag substrates (Ref 10). Also, some large Ag_3Sn plates appeared in solder matrix have reported in the Sn-Ag-Cu solder joints (Ref 11, 12). Lee et al. investigated the appearance of such large intermetallic compounds in the solder and pointed out a harmful effect on the mechanical properties of the solder joints (Ref 13). Figure 4 reveals that no Ag_3Sn precipitates appear in the Sn-20In-2.8Ag solder matrix. This result is consistent with the observation of Chiang (Ref 8) that the addition of In into the Sn-rich solder can suppress the formation of Ag_3Sn intermetallic compounds.

Figure 5 shows the morphology of intermetallic compounds in Sn-20In-2.8Ag solder BGA packages with immersion Ag pads after aging at 100 °C for various times. It can be seen that

the interfacial intermetallic compounds η-$(Cu_{0.98}Ag_{0.02})_6(Sn_{0.59}In_{0.41})_5$ formed during the reflow process have not grown obviously with the aging time, yet a small number of η-$(Cu_{0.98}Ag_{0.02})_6(Sn_{0.59}In_{0.41})_5$ intermetallic clusters float into the solder matrix after aging. The composition of the interfacial intermetallic compounds shows no change with the increase of aging time, while more intermetallic scallops float away from the solder pad. In addition, there is a slight coarsening of $(Ag_{0.94}Cu_{0.06})_2In$ in the solder matrix. Figure 6 shows the accelerated growth of the η-$(Cu_{0.98}Ag_{0.02})_6(Sn_{0.59}In_{0.41})_5$ intermetallic compounds with the aging time when the aging temperature is increased to 150 °C. It can also be observed that only the η-$(Cu_{0.98}Ag_{0.02})_6(Sn_{0.59}In_{0.41})_5$ intermetallic layer appears at the interface. For the Cu/Sn interfacial reactions,

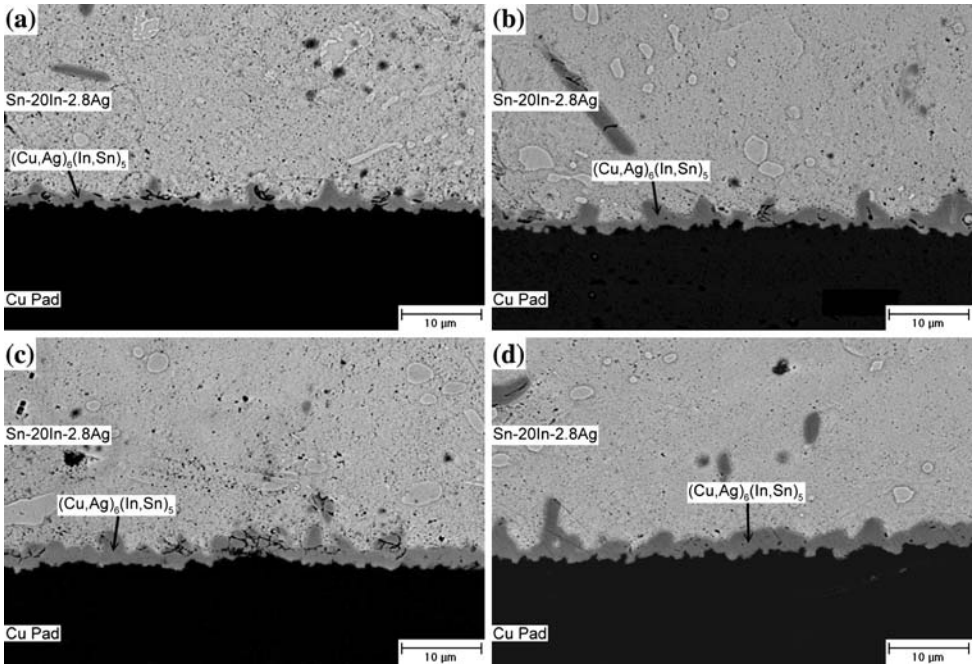

Fig. 5 Morphology of Sn-20In-2.8Ag solder balls and immersion Ag surface finish of Cu pads after aging at 100 °C for various time periods: (a) 100 h, (b) 500 h, (c) 700 h, and (d) 1000 h

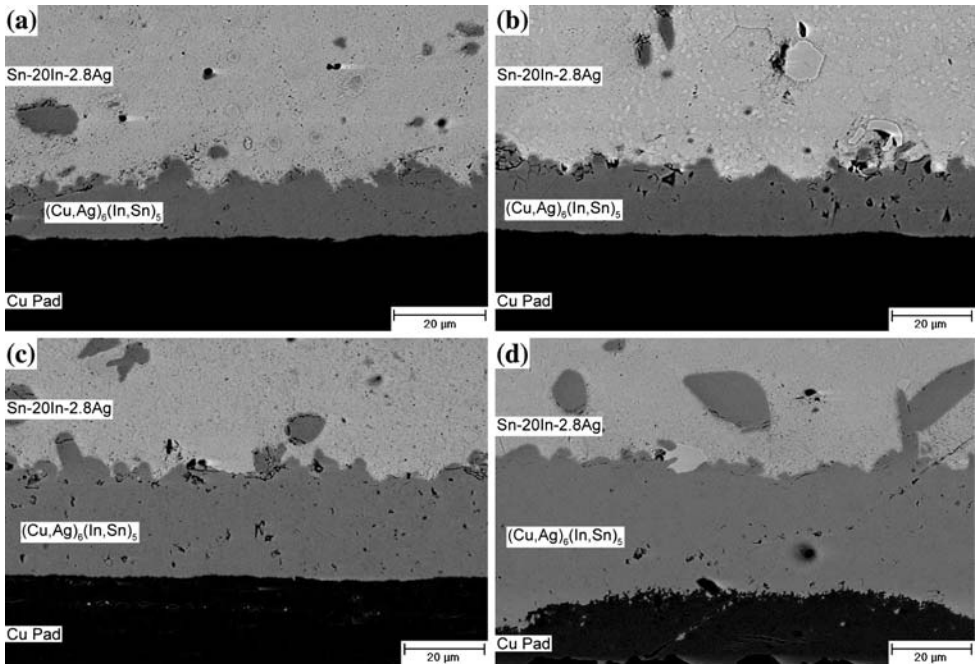

Fig. 6 Morphology of Sn-20In-2.8Ag solder balls and immersion Ag surface finish of Cu pads after aging at 150 °C for various times: (a) 100 h, (b) 500 h, (c) 700 h, and (d) 1000 h

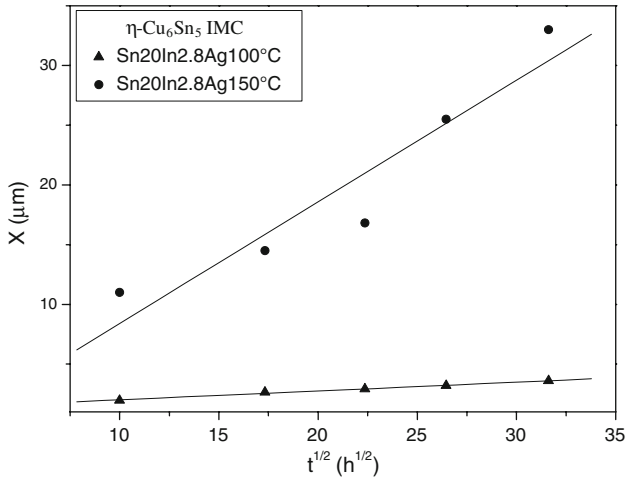

Fig. 7 Growth thickness (X) of the intermetallic compound η-IMC during the aging of the Sn-20In-2.8Ag with immersion Ag surface finish at 100 and 150 °C versus the square root of time ($t^{1/2}$)

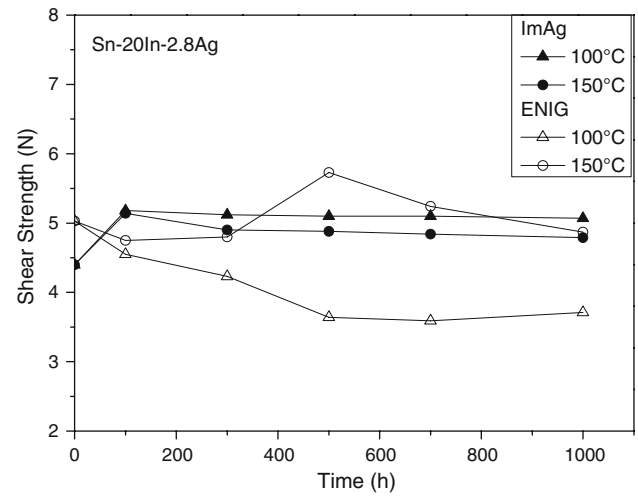

Fig. 8 The ball shear strengths of the Sn-20In-2.8Ag solder BGA packages with immersion Ag surface finish (ImAg) under various aging conditions. For comparison, the results of the ENIG-surface finished Sn-20In-2.8Ag packages measured in the prior study (Ref 9) are given in this figure

an ε-Cu_3Sn intermetallic phase has often been reported to form between the η-Cu_6Sn_5 intermetallic layer and the Cu pad. Chih and Chuang found that during the aging process at 150 °C for an immersion Ag surface finished Sn-3.5Ag solder BGA package (Ref 14), an ε-Cu_3Sn intermetallic layer appeared after the formation of η-Cu_6Sn_5 intermetallics. In addition, many Kirkendall voids were observed in the interior of the ε-Cu_3Sn layer. The appearance of ε-Cu_3Sn intermetallic compounds accompanying Kirkendall voids has also been reported in Sn-3.5Ag-0.5Cu solder joints with Ag/Cu pads (Ref 15). The inhibition of the ε-Cu_3Sn intermetallic phase seems to be a beneficial effect of the addition of indium on the immersion Ag surface finished Sn-20In-2.8Ag solder package.

The thickness (X) of the η-$(Cu_{0.98}Ag_{0.02})_6(Sn_{0.59}In_{0.41})_5$ intermetallic compounds formed during the aging of Sn-20In-2.8Ag solder BGA packages with Ag/Cu pads at 100 and 150 °C is plotted versus the square root of reaction time ($t^{1/2}$) in Fig. 7. The curves exhibit a linear relation, which indicates that the growth of η-$(Cu_{0.98}Ag_{0.02})_6(Sn_{0.59}In_{0.41})_5$ intermetallics is diffusion-controlled. Ball shear strengths of the immersion Ag surface finished Sn-20In-2.8Ag solder BGA packages after aging at 100 and 150 °C are shown in Fig. 8. For comparison, the results of ball shear tests performed on Sn-20In-2.8Ag BGA packages with ENIG-surface finish (Au/Ni/Cu pads) in our prior study (Ref 9) are also given in Fig. 8. It is evident that the bonding strength of the as-reflowed Sn-20In-2.8Ag solder joints (4.4 N) with Ag/Cu pads is lower than that of the ENIG-surface finished packages (5.0 N). After aging at 100 and 150 °C for 1000 h, the bonding strengths of Sn-20In-2.8Ag solder joints with Au/Ni/Cu pads decline to 4.8 N and 3.7 N, respectively. However, the ball shear strength of Sn-20In-2.8Ag solder joints after aging at 100 °C for 100 h climbs to 5.18 N and remains almost constant with the increase of the aging time. Aging at 150 °C for 100 h also causes an increase of the ball shear strength to 5.14 N, while it declines slightly to 4.8 N for a longer aging time. Figure 9 shows the typical fractography of reflowed Sn-20In-2.8Ag solder joints in BGA packages after ball shear tests, which have mostly ruptured along the interface between $(Cu_{0.98}Ag_{0.02})_6(Sn_{0.59}In_{0.41})_5$ intermetallics and the solder pad. With further aging, more ductile fractured dimples throughout the matrix can be observed in the fractography, as shown in Fig. 10. The results imply that the appearance of interfacial intermetallic compounds during aging processes at 100 and 150 °C leads to a more satisfactory reaction between Sn-20In-2.8Ag solder and the Cu pad, which transfers the fracture path from solder/pad interfaces to solder matrix.

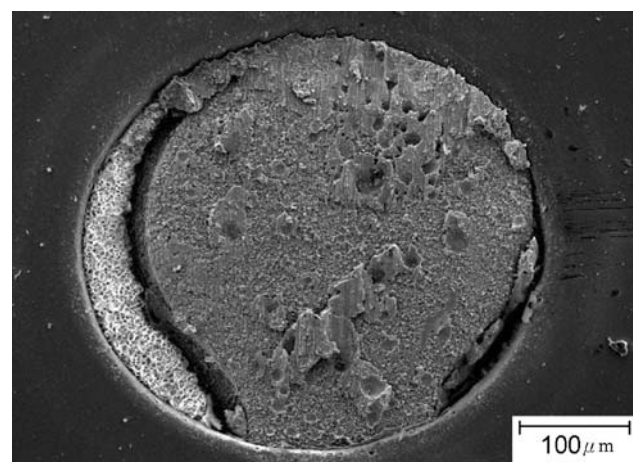

Fig. 9 Fractography of the as-reflowed Sn-20In-2.8Ag solder joints in BGA packages with immersion Ag surface finish after ball shear test

4. Conclusions

After the reflow of Sn-20In-2.8Ag solder joints on immersion Ag surface finished Cu pads in ball grid array (BGA) packages, the Ag thin film has dissolved completely and caused the formation of η-$(Cu_{0.98}Ag_{0.02})_6(Sn_{0.59}In_{0.41})_5$ at the interfaces between the solder balls and the Cu pads. A great number of island-like precipitates with a composition of $(Ag_{0.94}Cu_{0.06})_2In$ are embedded in the Sn-rich matrix. After prolonged

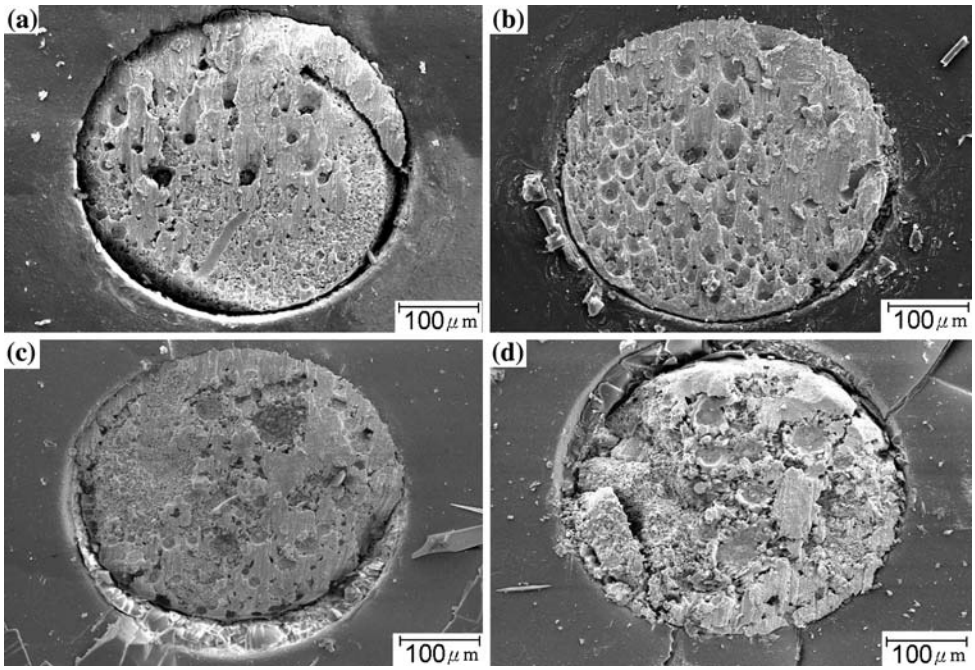

Fig. 10 Fractography of the aged Sn-20In-2.8Ag solder joints in BGA packages with immersion Ag surface finish after ball shear tests: (a) 100 °C, 100 h, (b) 100 °C, 1000 h, (c) 150 °C, 100 h, and (d) 150 °C, 1000 h

aging at 150 °C, a η-$(Cu_{0.98}Ag_{0.02})_6(Sn_{0.59}In_{0.41})_5$ intermetallic layer appears at the interface and grows rapidly. The occurrence of ε-Cu_3Sn phase has been inhibited on the immersion Ag surface finished by the addition of indium to Sn-20In-2.8Ag solder. The growth of η-$(Cu_{0.98}Ag_{0.02})_6(Sn_{0.59}In_{0.41})_5$ follows a linear relation, indicating that the reaction is diffusion-controlled. The ball shear strength of the immersion Ag surface finished Sn-20In-2.8Ag solder BGA packages after aging at 100 and 150 °C increases from 4.4 N (reflowed state) to 5.18 N and 5.14 N, respectively. The increase of bonding strength for solder joints in this case is attributed to the more satisfactory interfacial reaction between the Sn-20In-2.8Ag solder and the Cu pad during the aging process.

Acknowledgments

The authors sincerely acknowledge the financial support for this research from National Taiwan University under Grant No. 96R-0210 and the National Science Council, Taiwan, under Grant No. NSC. 93-2216-E002-024.

References

1. A.M. Minor and J.W. Morris, Inhibiting Growth of the $Au_{0.5}Ni_{0.5}Sn_4$ Intermetallic Layer in Pb-Sn Solder Joints Reflowed on Au/Ni Metallization, *J. Electron. Mater.*, 2000, **29**(10), p 1170–1174
2. Z. Mei, M. Kaufmann, A. Eslambolchi, and P. Johnson, Brittle Interfacial Fracture of PBGA Packages Soldered on Electroless Nickel/Immersion Gold, *IEEE Electron. Compon. and Technol. Conf.*, 1998, p 952–961
3. J.H. Lau, C.P. Wong, N.C. Lee, and S.W. Ricky Lee, *Electronics Manufacturing with Lead-free, Halogen-free Conductive-Adhesive Materials,* McGraw-Hill Handbooks, 2003
4. J. Glazer, Metallurgy of Low Temperature Pb-free Solders for Electronics Assembly, *Int. Mater. Rev.*, 1995, **40**(2), p 65–93
5. Z. Mei and J.W. Morris, Characterization of Eutectic Sn-Bi Solder Joints, *J. Electron. Mater.*, 1992, **21**(6), p 599–607
6. K. Shimizn, T. NaKanishi, K. Karasawa, K. Hashimoto, and K. Niwa, Solder Joint Reliability of Indium-Alloy Interconnection, *J. Electron. Mater.*, 1995, **24**(1), p 39–45
7. T.H. Chuang, K.W. Huang, and W.H. Lin, Mechanisms for the Intermetallic Formation During the Sn-20In-2.8Ag/Ni Soldering Reactions, *J. Electron. Mater.*, 2004, **33**(4), p 374–382
8. M.J. Chiang and T.H. Chuang, Interfacial Reaction Between Liquid Sn-20In-2.8Ag Solder and Ag Substrate, *Z. Metallkd.*, 2002, **93**(12), p 1194–1198
9. H.M. Wu, F.C. Wu, and T.H. Chuang, Intermetallic Reactions in a Sn-20In–2.8Ag Solder Ball-Grid-Array Package with Au/Ni/Cu Pads, *J. Electron. Mater.*, 2005, **34**(11), p 1385–1390
10. T.L. Su, L.C. Tsao, S.Y. Chang, and T.H. Chuang, Interfacial Reactions of Liquid Sn and Sn-3.5Ag Solders with Ag Thick Films, *J. Mater. Eng. Perform.*, 2002, **11**(5), p 481–486
11. D.W. Henderson, T. Gosselin, A. Sarkhel, S.K. Kang, W.K. Choi, D.Y. Shih, C. Goldsmith, and K.J. Puttlitz, Ag_3Sn Plate Formation in the Solidification of Near Ternary Eutectic Sn-Ag-Cu Alloys, *J. Mater. Res.*, 2002, **17**(11), p 2775–2778
12. M.D. Cheng, S.Y. Chang, S.F. Yen, and T.H. Chuang, Intermetallic Compounds Formed During the Reflow and Aging of Sn-3.8Ag-0.7Cu and Sn-20In-2Ag-0.5Cu Solder Ball Grid Array Packages, *J. Electron. Mater.*, 2004, **33**(3), p 171–180
13. T.Y. Lee, W.J. Choi, K.N. Tu, J.W. Jang, S.M. Kuo, J.K. Lin, D.R. Frear, K. Zeng, and J.K. Kivilathi, Morphology, Kinetics, and Thermodynamics of Solid-State Aging of Eutectic SnPb and Pb-free Solders (Sn-3.5Ag, Sn-3.8Ag-0.7Cu and Sn-0.7Cu) on Cu, *J. Mater. Res.*, 2002, **17**(2), p 291–301
14. C.C. Chi and T.H. Chuang, Intermetallic Reactions in Sn-3.5Ag Solder Ball Grid Array Packages with Ag/Cu and Au/Ni/Cu Pads, *J. Electron. Mater.*, 2006, **35**(3), p 471–478
15. T.H. Chuang, S.F. Yen, and H.M. Wu, Intermetallic Formation in Sn3Ag0.5Cu and Sn3Ag0.5Cu0.06Ni0.01Ge Solder BGA Packages with Immersion Ag Surface Finish, *J. Electron. Mater.*, 2006, **35**(2), p 310–318